(3) Gates, J. A.; Tillett, D. M.; White, D. E.; Wood, R. H. *J. Chem. Thermodyn.* **1987**, *19*, 131.
(4) White, D. E.; Gates, J. A.; Wood, R. H. *J. Chem. Thermodyn.* **1987**, *19*, 493, 1037.
(5) White, D. E.; Doberstein, A. L.; Gates, J. A.; Tillett, D. M.; Wood, R. H. *J. Chem. Thermodyn.* **1987**, *19*, 251.
(6) White, D. E.; Ryan, M. A.; Cavalucci Armstrong, M. A.; Gates, J. A. *J. Chem. Thermodyn.* **1987**, *19*, 1023.
(7) Cobble, J. W.; Murray, R. C., Jr. *Discuss. Faraday Soc.* **1977**, *64*, 144.
(8) Cobble, J. W.; Murray, R. W., Jr.; Sen, U. *Nature* **1981**, *291*, 566.
(9) Helgeson, H. C.; Kirkham, D. H. *Abstracts of Papers*, 174th meeting of American Chemical Society, New Orleans, LA, March 1977.
(10) Helgeson, H. C.; Kirkham, D. H.; Flowers, D. C. *Am. J. Sci.* **1981**, *281*, 1249.
(11) Wood, R. H.; Quint, J. R.; Grolier, J.-P. *J. Phys. Chem.* **1981**, *85*, 3944.
(12) Wood, R. H.; Quint, J. R. *J. Chem. Thermodyn.* **1982**, *14*, 1069.
(13) Wheeler, J. C. *Ber. Bunsen-Ges. Phys. Chem.* **1972**, *76*, 308.
(14) Gates, J. A.; Wood, R. H.; Quint, J. R. *J. Phys. Chem.* **1982**, *86*, 4948.
(15) Chang, R. F.; Morrison, G.; Levelt-Sengers, J. M. H. *J. Phys. Chem.* **1984**, *88*, 3389.
(16) Smith-Magowan, D. Ph.D. Dissertation, University of Delaware, May 1980.
(17) Karapet'yants, M. Kh.; Vasilëv, D. A.; Sanaev, E. S. *Russ. J. Phys. Chem.* **1977**, *51*, 1281.
(18) White, D. E.; Wood, R. H. *J. Solution Chem.* **1982**, *11*, 223.
(19) Fortier, J.-L.; Benson, G. C.; Picker, P. *J. Chem. Thermodyn.* **1976**, *8*, 289.
(20) Bernaducci, E. E.; Morss, L. R.; Miksztal, A. R. *J. Solution Chem.* **1979**, *8*, 717.
(21) Gates, J. A. Ph.D. Dissertation, University of Delaware, Newark, January 1985.
(22) Uematsu, M.; Franck, E. U. *J. Phys. Chem. Ref. Data* **1980**, *9*, 1291.
(23) Haar, L.; Gallagher, J. S.; Kell, G. S. *NBS/NRC Steam Tables*; Hemisphere: Washington, DC, 1984.
(24) Saluja, P. P. S.; Pitzer, K. S.; Phutela, R. C. *Can. J. Chem.* **1986**, *64*, 1328.
(25) Mains, G. J.; Sarson, J. W.; Hepler, L. G. *J. Phys. Chem.* **1984**, *88*, 1257.

Received for review June 23, 1987. Accepted February 16, 1988. We thank the Electric Power Research Institute (contract No. RP1167-4) for their support of this work.

# Solubility Relationship in the System $NaNO_3$–$NH_4NO_3$–Urea–$H_2O$ at 0 °C

**Yong K. Kim,* Joseph W. Williard, and Alva W. Frazier**

*Division of Research, Tennessee Valley Authority, National Fertilizer Development Center, Muscle Shoals, Alabama 35660*

**The solubilities of the various components were determined in the system $NaNO_3$–$NH_4NO_3$–urea–$H_2O$ at 0 °C. The maximum nitrogen in solution contained the minimum amount of $NaNO_3$. A solution of 30.3 wt % nitrogen was composed of 38.2% $NH_4NO_3$, 9.0% $NaNO_3$, 33.0% urea, and 19.8% $H_2O$. The saturation solubility data were plotted on a water-free basis, and isoconcentration lines (lines of constant nitrogen content) were drawn to exhibit the graph in an easily interpretable form. A compound, $NaNO_3 \cdot 2urea \cdot 2H_2O$, that had not been previously described was found in the system, and all petrographic data were determined.**

Previous work in the field of nitrogen solubility has been mainly with two nitrogen-containing compounds. Polosin and Tarasova (*1*) studied the system $NaNO_3$–urea–$H_2O$; Sokolov (*2*) published solubility data for the system urea–$NH_4NO_3$–$H_2O$; and Seidell (*3*) published the solubility relationship for the system $NH_4NO_3$–$NaNO_3$–$H_2O$. Several investigators have reported eutectic information for the system $NaNO_3$–$NH_4NO_3$–urea (*4*–*6*), where the ternary eutectic mixtures have shown the eutectic temperature to be about 35–39 °C. There were no solubility data available for the four-component system $NaNO_3$–$NH_4NO_3$–urea–$H_2O$, which is of interest for the utilization of byproduct sodium nitrate as a fluid fertilizer. This solubility study was initiated to determine the nitrogen concentration at all combinations of the three input compounds at 0 °C. This temperature (0 °C) was selected because it is used as a standard by the fertilizer industry to evaluate fluid products which require storage during winter months.

## Material and Experimental Procedures

The equilibrium solutions used to determine the solubility in the $NaNO_3$–$NH_4NO_3$–urea–$H_2O$ system were prepared from reagent chemicals without further purification. Thirty-four mixtures of 100 g each were prepared with urea in the concentration range 6–40%, ammonium nitrate in the range 5–50%, and sodium nitrate in the range 4–43%. These solutions were equilibrated in a cold room thermostated at 0 ± 0.5 °C and shaken periodically. After 24 h those cells that contained no solids were treated with 10% each of the original salt mixtures and equilibration was continued. This procedure of adding 10% of the original salts was repeated until all the solutions were saturated with at least one solid phase. Equilibration was continued for 2 weeks after a solid phase became stable in each solution. Samples of the solid phases then were taken and filtered on a fritted crucible that had been cooled to 0 °C. The solid phases were identified by polarizing light microscopy (PLM). The total and ammoniacal nitrogen in the liquid phase were determined by Association of Official Analytical Chemists (AOAC) methods (*7*), the nitrate and urea nitrogen were determined by high-performance liquid chromatography (HPLC, unpublished TVA method), and sodium was determined by flame emission spectroscopy.

## Results and Discussion

Solubility data for the system $NaNO_3$–$NH_4NO_3$–urea–$H_2O$ at 0 °C are given in Table I. Since total nitrogen and its three forms (ammonia N, nitrate N, and urea N) were measured individually, the difference ($\Delta N$) between the total nitrogen and the sum of the three nitrogen forms can serve as a check of the deviation in the chemical analysis. The highest deviation occurred in experiment 21, with a $\Delta N$ of 0.34. All other tests have a $\Delta N$ value of about 0.15, indicating that the nitrogen determinations were reliable.

The distribution of nitrogen among the different forms of nitrogen sources was calculated from the individual nitrogen values and is listed in Table I. Also, the composition of the saturated solution was calculated from the individual nitrogen data, and water was measured as the difference between the weight of solution and solutes. Finally, the composition of the solutes in the saturated solution based on a water-free condition was calculated from the solution composition and is given as

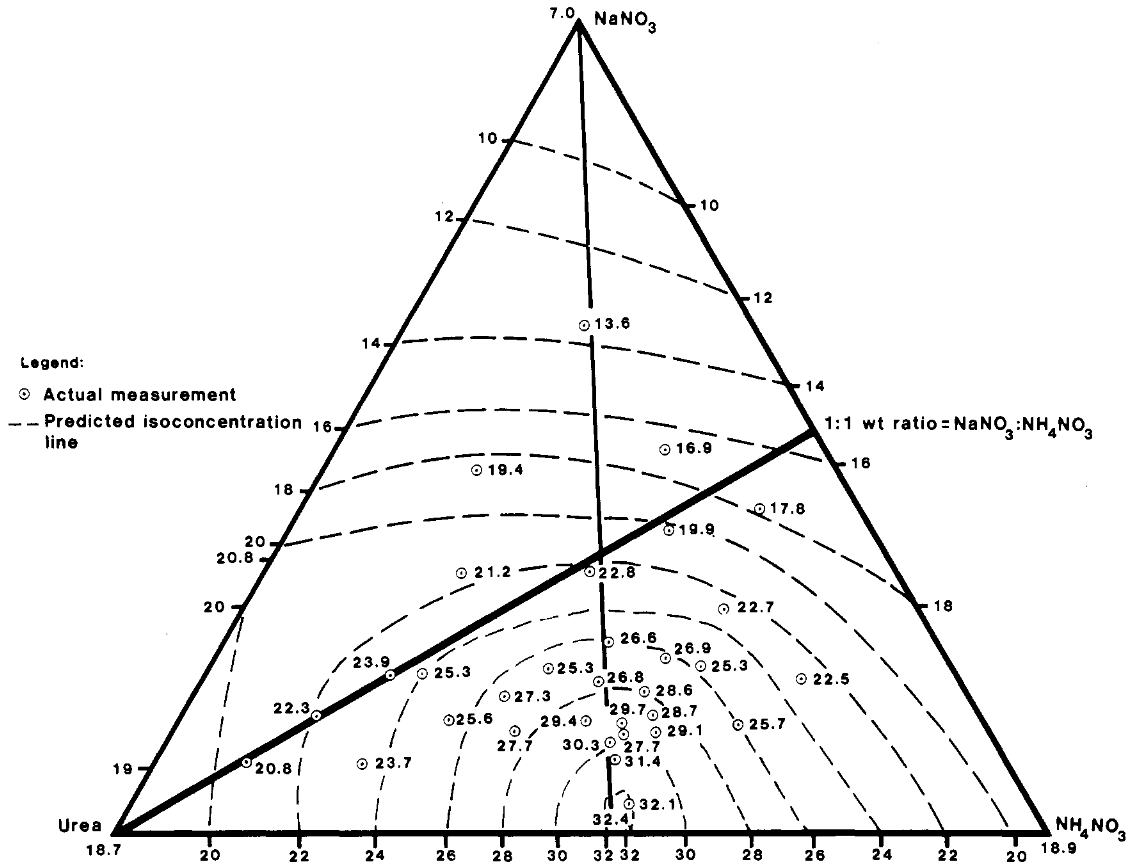

**Figure 1.** Solubility relationship in the system $NaNO_3$–$NH_4NO_3$–urea–$H_2O$ at 0 °C (numbers denote total nitrogen concentration, wt %, in saturated solution).

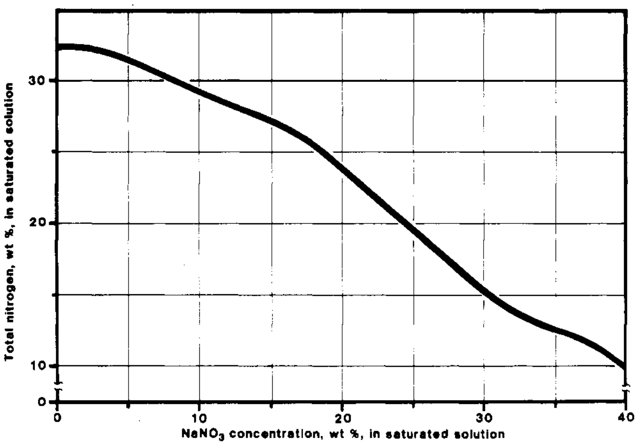

**Figure 2.** Relationship between total nitrogen content and $NaNO_3$ when weight ratio $NH_4NO_3$:urea is 54:46.

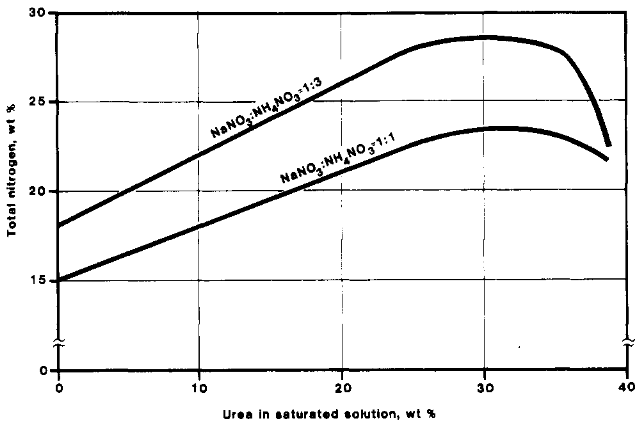

**Figure 3.** Variation of total nitrogen content in saturated solution when urea content is increased from zero to 39 wt % and weight ratio $NaNO_3$:$NH_4NO_3$ is 1:1 or 1:3.

"distribution of solute" in Table I. The solid phases in equilibrium with the saturated solution were identified by PLM and are listed in Table I.

Saturation solubility data are plotted on a water-free basis in Figure 1. The relative distribution of the three compounds in the saturated solution phase was plotted as a triangular graph by using the solute distribution data from Table I. The numbers on Figure 1 are the total nitrogen (actual weight percent) in each saturated solution (not water-free basis). The nitrogen contents in the three-component systems (shown as the edges of the triangle) were derived from the following published data after an appropriate interpolation: $NaNO_3$–$NH_4NO_3$–$H_2O$ from Seidell (*3*), $NaNO_3$–urea–$H_2O$ from Polosin and Tarasova (*1*), and $NH_4NO_3$–urea–$H_2O$ from Sokolov (*2*). The water content in the solution can be calculated from total nitrogen and the composition of the solutes. Since the large numbers of experimental data are distributed in a whole region, isoconcentration lines (dotted lines = lines of constant nitrogen content) were drawn to exhibit the graph in an easily interpretable form.

The highest isoconcentration line of 32% N is located at about a 1:1 weight mixture of $NH_4NO_3$ and urea, with very little $NaNO_3$. When the saturation composition moves away from this highest nitrogen region in any direction, the total nitrogen concentration will decrease. The lowest nitrogen concentration can be seen at the top of the triangular graph where $NaNO_3$ is the only solute. The highest nitrogen-containing solution for the system $NH_4NO_3$–urea–$H_2O$ occurs at 46% urea and 54% $NH_4NO_3$ (dry basis). A line was drawn from this point to the top of the triangular graph (100% $NaNO_3$), as shown in Figure 1.

The change in total nitrogen concentration along the line was interpolated from the isoconcentration lines and plotted in Figure 2. As the sodium nitrate concentration increases in the sat-

**Table I. Solubility in the System $NaNO_3$–$NH_4NO_3$–Urea–$H_2O$ at 0 °C**

| | experiment no. | | | | | | | | | | | | | |
|---|---|---|---|---|---|---|---|---|---|---|---|---|---|---|
| | 1 | 2 | 3 | 4 | 5 | 6 | 7 | 8 | 9 | 10 | 11 | 12 | 13 | 14 |
| concn in soln, wt % | | | | | | | | | | | | | | |
| total nitrogen | 30.30 | 31.20 | 29.70 | 26.60 | 29.40 | 28.60 | 31.40 | 29.10 | 27.70 | 27.70 | 27.30 | 29.70 | 28.70 | 25.30 |
| ammonia nitrogen | 6.68 | 6.95 | 6.93 | 5.50 | 5.95 | 6.65 | 7.01 | 7.11 | 6.10 | 4.59 | 4.20 | 6.65 | 6.93 | 6.80 |
| nitrate nitrogen | 8.16 | 8.36 | 8.67 | 8.50 | 7.75 | 8.98 | 8.24 | 8.69 | 7.59 | 6.12 | 6.23 | 8.47 | 8.85 | 9.58 |
| urea nitrogen | 15.40 | 16.00 | 14.00 | 12.60 | 15.50 | 12.80 | 16.00 | 13.20 | 13.00 | 16.80 | 16.70 | 14.30 | 12.90 | 8.75 |
| sodium | 1.89 | 2.08 | 2.45 | 4.52 | 2.46 | 3.72 | 1.69 | 2.57 | 2.09 | 2.32 | 2.80 | 1.83 | 2.40 | 3.83 |
| $\Delta N^a$ | 0.06 | -0.11 | 0.10 | 0.00 | 0.20 | 0.17 | 0.15 | 0.10 | 1.01 | 0.19 | 0.17 | 0.28 | 0.02 | 0.17 |
| composn of soln, wt % | | | | | | | | | | | | | | |
| ammonium nitrate | 38.17 | 39.17 | 39.60 | 31.43 | 34.00 | 38.00 | 40.06 | 40.63 | 34.86 | 26.23 | 24.00 | 38.00 | 39.60 | 38.86 |
| sodium nitrate | 8.97 | 8.55 | 10.55 | 18.18 | 10.91 | 14.12 | 7.45 | 9.58 | 9.03 | 9.27 | 12.30 | 11.03 | 11.64 | 16.85 |
| urea | 33.01 | 34.30 | 30.01 | 27.01 | 33.23 | 27.44 | 34.30 | 28.30 | 27.87 | 36.01 | 35.80 | 30.65 | 27.65 | 18.76 |
| water | 19.85 | 17.44 | 19.84 | 23.38 | 21.86 | 20.44 | 18.19 | 21.50 | 28.25 | 28.49 | 27.90 | 20.32 | 21.11 | 25.54 |
| distribn of solute, wt % | | | | | | | | | | | | | | |
| ammonium nitrate | 47.62 | 48.10 | 49.40 | 41.02 | 43.51 | 42.76 | 48.96 | 51.76 | 48.58 | 56.68 | 33.29 | 47.69 | 50.20 | 52.18 |
| sodium nitrate | 11.19 | 10.35 | 13.16 | 23.73 | 13.96 | 17.75 | 9.11 | 12.20 | 12.58 | 12.97 | 17.06 | 13.84 | 14.75 | 22.63 |
| urea | 41.19 | 41.54 | 37.44 | 35.25 | 42.52 | 34.49 | 41.92 | 36.05 | 38.84 | 50.36 | 49.65 | 38.47 | 35.05 | 25.19 |
| solid phase$^b$ | U, A | U, A, S, S·2U, UK2 | A, S | S | A, S, S·2U, UK1 | A, UK2 | S, S·2U | A | A | U | U, S | S·2U | S, S·2U | A, S, UK2 |

[a] Difference between total nitrogen and sum of ammonia N, nitrate N, and urea N. [b] U = urea, A = ammonium nitrate, S = sodium

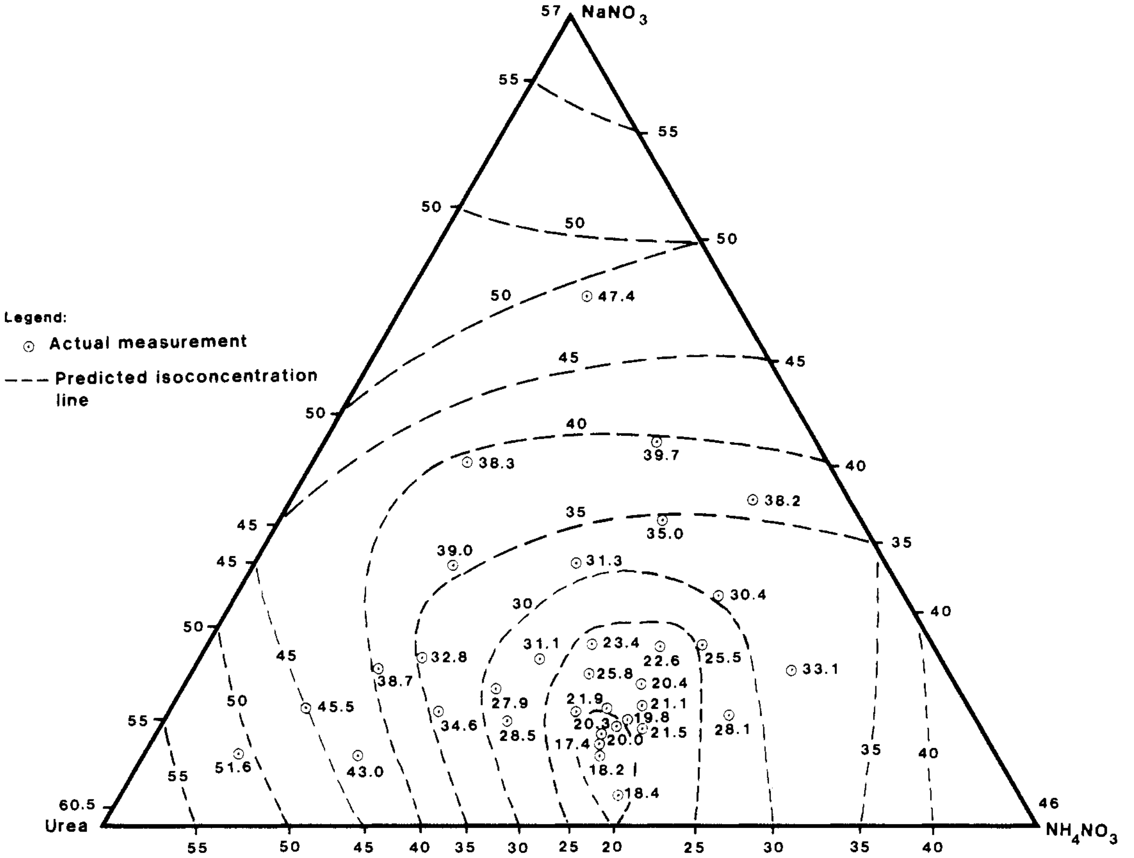

**Figure 4.** Water content (wt %) in saturated solutions in the system $NaNO_3$–$NH_4NO_3$–urea–$H_2O$ system at 0 °C.

urated solution from zero to 2–3%, almost no change is predicted and the total nitrogen concentration remains at 32%. A further increase of $NaNO_3$ up to 18% in the saturated solution phase makes the total nitrogen concentration decrease at a rate of 0.45% N decrease per 1% $NaNO_3$ increase. Additional increases from 18 to 31% cause the total nitrogen decrease rate to almost double to 0.85. Thereafter, the nitrogen decrease rate is lower, but increases again at the extreme top range of Figure 1.

Starting with a mixture of $NaNO_3$ and $NH_4NO_3$, a prediction can be made of the total nitrogen content in a saturated solution containing varying amounts of urea. For example, using a 1:1 mixture of $NaNO_3$:$NH_4NO_3$, a line can be drawn from the midpoint of $NaNO_3$ and $NH_4NO_3$ to the lower left corner at 100% urea, as shown in Figure 1. The variation of total nitrogen along this line was interpolated from the isoconcentration lines and plotted in Figure 3 (lower line). The total nitrogen concentration gradually increases from 15 to 23% as the urea concentration increases from zero to 30%. A further increase of urea will not increase the total nitrogen; it actually decreases at higher urea concentrations.

When the starting mixture has a 1:3 weight ratio of $NaNO_3$:$NH_4NO_3$, the total nitrogen concentration can be predicted from the isoconcentration values along the line from the 25:75 point of $NaNO_3$:$NH_4NO_3$ to the urea apex. Again, these interpolated values are plotted in Figure 3 (upper line). The shape

| experiment no. | | | | | | | | | | | | | | | | | | | |
|---|---|---|---|---|---|---|---|---|---|---|---|---|---|---|---|---|---|---|---|
| 15 | 16 | 17 | 18 | 19 | 20 | 21 | 22 | 23 | 24 | 25 | 26 | 27 | 28 | 29 | 30 | 31 | 32 | 33 | 34 |
| 26.90 | 25.70 | 17.80 | 19.90 | 22.80 | 25.30 | 23.90 | 22.30 | 20.80 | 22.50 | 22.70 | 26.80 | 25.60 | 23.70 | 16.90 | 13.60 | 19.40 | 21.20 | 25.30 | 32.10 |
| 6.50 | 7.53 | 5.30 | 4.60 | 4.18 | 4.38 | 2.14 | 1.37 | 0.85 | 7.47 | 6.26 | 5.53 | 3.31 | 2.27 | 3.72 | 1.76 | 1.80 | 2.28 | 2.80 | 7.60 |
| 9.28 | 9.14 | 9.38 | 8.64 | 7.83 | 6.71 | 4.12 | 2.71 | 1.56 | 9.57 | 9.45 | 7.82 | 4.82 | 3.10 | 8.42 | 7.16 | 6.35 | 5.50 | 5.10 | 8.10 |
| 10.90 | 8.94 | 3.15 | 6.64 | 10.60 | 13.90 | 17.30 | 18.00 | 18.30 | 5.34 | 6.78 | 13.40 | 17.40 | 18.20 | 4.92 | 4.57 | 11.10 | 13.30 | 17.40 | 16.40 |
| 3.59 | 2.31 | 6.50 | 6.09 | 5.78 | 3.88 | 3.29 | 2.23 | 1.12 | 3.05 | 5.26 | 3.50 | 2.44 | 1.50 | 7.29 | 8.76 | 7.29 | 5.14 | | |
| 0.22 | 0.09 | −0.03 | 0.02 | 0.19 | 0.31 | 0.34 | 0.22 | 0.09 | 0.12 | 0.21 | 0.05 | 0.07 | 0.13 | −0.16 | 0.11 | 0.15 | 0.12 | 0.00 | 0.00 |
| 37.14 | 43.03 | 30.29 | 26.29 | 23.89 | 25.03 | 12.23 | 7.83 | 4.86 | 42.69 | 35.77 | 31.60 | 18.91 | 12.97 | 21.26 | 10.06 | 10.29 | 13.03 | 16.00 | 43.43 |
| 16.85 | 9.76 | 24.73 | 24.48 | 22.12 | 14.12 | 12.00 | 8.12 | 4.30 | 12.73 | 19.33 | 13.88 | 9.15 | 5.03 | 28.48 | 32.73 | 27.58 | 19.52 | 13.94 | 3.03 |
| 23.37 | 19.16 | 6.75 | 14.23 | 22.72 | 29.80 | 37.08 | 38.59 | 39.23 | 11.45 | 14.53 | 28.72 | 37.30 | 39.01 | 10.55 | 9.80 | 23.79 | 28.51 | 37.30 | 35.16 |
| 22.64 | 28.05 | 38.23 | 35.00 | 31.27 | 31.05 | 38.69 | 43.47 | 51.61 | 33.14 | 30.36 | 25.80 | 34.64 | 42.98 | 39.71 | 47.42 | 38.34 | 38.95 | 32.76 | 18.39 |
| 48.01 | 59.80 | 49.03 | 40.44 | 34.75 | 36.30 | 19.94 | 14.36 | 10.04 | 63.84 | 51.37 | 42.59 | 28.94 | 22.75 | 35.26 | 19.13 | 16.68 | 21.34 | 23.80 | 53.21 |
| 21.78 | 13.56 | 40.03 | 37.67 | 32.19 | 20.48 | 19.57 | 14.89 | 8.89 | 19.04 | 27.76 | 18.70 | 14.00 | 8.82 | 47.25 | 62.24 | 44.73 | 31.96 | 20.73 | 3.71 |
| 30.20 | 26.64 | 10.93 | 21.90 | 33.06 | 43.22 | 60.48 | 70.75 | 81.07 | 17.12 | 20.87 | 38.71 | 57.06 | 68.43 | 17.49 | 18.63 | 38.59 | 46.70 | 55.47 | 43.08 |
| A, S | A | S, A | S | S | S·2U, UK2 | U | U | U | A | S | S·2U, UK2 | U | U | S | S | S | S·2U | U | A |

nitrate, S·2U = $NaNO_3 \cdot 2CO(NH_2)_2 \cdot 2H_2O$, UK1 = unknown compound, UK2 = unknown compound.

of the total nitrogen variation curve as a function of increasing urea is similar and the lines are essentially parallel, with the 1:3 material (upper line) having an almost 3–5% higher nitrogen concentration than that of the 1:1 mixture.

These results demonstrate that a more acceptable high-analysis, nitrogen-containing solution can be made at lower ratios of $NaNO_3$:$NH_4NO_3$. These low ratios impede the goal of using large quantities of $NaNO_3$. The water content in saturation solution as a function of $NaNO_3$, $NH_4NO_3$, and urea is plotted in Figure 4. The dashed lines representing water content were estimated from the literature and this study. The isoconcentration of water will provide needed data when formulating solutions from $NaNO_3$, $NH_4NO_3$, and urea.

The solid phases in the saturated solution were analyzed microscopically to identify the saturating compounds. The three input compounds ($NaNO_3$, $NH_4NO_3$, and urea) are well-known and readily identified as the only saturating solids in large areas of the system where each has a stable stability field, as shown in Figure 5. Three additional compounds were encountered at 0 °C in the composition region represented by the shaded area of Figure 5. Previous studies indicated that only one compound—$NaNO_3 \cdot CO(NH_2)_2 \cdot H_2O$ (*8*) or a series of compounds—would exist in this system. A new compound was identified chemically as $NaNO_3 \cdot 2CO(NH_2)_2 \cdot 2H_2O$ and is stable at room temperature. Optical characterization shows that $NaNO_3 \cdot 2CO(NH_2)_2 \cdot 2H_2O$ crystallizes as monoclinic, $2/m$ plate crystals tabular on (010) and elongated along $c$. The crystals exhibit contact twinning with the (100) as the composition plane. Optically, $X \wedge C = 28°$ in acute $\beta$; $Y = b$, $d_{\text{calcd}} = 1.55$, $2V_{\text{calcd}} = 38°$, $N_\alpha = 1.395$, $N_\beta = 1.545$, and $N_\lambda = 1.566$.

## Conclusions

Solubility relationships in the system $NaNO_3$–$NH_4NO_3$–urea–$H_2O$ at 0 °C were studied. Since a full-fledged phase system was not attempted, the data represent solubility measurements only. The results indicate that high-nitrogen-containing solutions can be produced by a proper combination of these three nitrogen compounds. For example, a solution containing about 30% nitrogen can be produced by incorporation of 8% $NaNO_3$ in a 46% urea:54% $NH_4NO_3$ solution (UAN). Any addition of $NaNO_3$ will decrease the total nitrogen concentration in the saturated solutions. Increasing total nitrogen and $NaNO_3$ indicates that one inversely affects the other. Therefore, the selection of optimum conditions (a balance between high nitrogen or high $NaNO_3$) can be achieved by using the solubility data presented here. The compromised condition will fulfill two objectives: the utilization of $NaNO_3$ and the production of nitrogen solutions for plant growth.

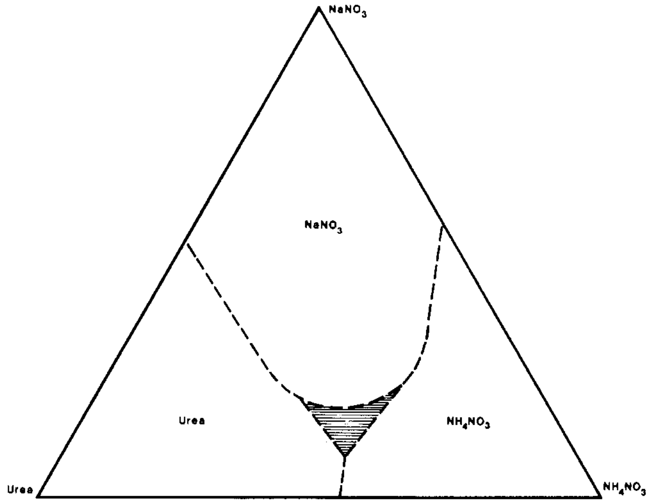

**Figure 5.** Distribution of precipitating solid phase for the system $NaNO_3$–$NH_4NO_3$–urea–$H_2O$ at 0 °C.

**Registry No.** $NaNO_3 \cdot 2urea \cdot 2H_2O$, 114719-56-1; $NaNO_3$, 7631-99-4; $NH_4NO_3$, 6484-52-2; urea, 57-13-6.

## Literature Cited

(1) Polosin, V. A.; Tarasova, N. N. *Dokl. TSKhA* **1956**, *22*, 398–404.
(2) Sokolov, V. A. *J. Gen. Chem.* (*USSR*) **1939**, *9*, 753–758.
(3) Seidell, A. *Solubilities of Inorganic and Metal Organic Compounds*; American Cyanamid Co.: Stanford, 1958; p 715.
(4) Campbell, A. N.; Campbell, A. J. R. *Can. J. Res.* **1947**, *25*, 90–100.
(5) Howells, W. J. *J. Chem. Soc.* **1930**, 2010–2017.
(6) Nogoev, K.; Bergman, A. G. *Zh. Prikl. Khim.* **1963**, *36*, 1680–1686.
(7) Association of Official Analytical Chemists. *Official Methods of Analysis of AOAC*; Association of Official Analytical Chemists: Arlington, VA, 1984.
(8) Polosin, V. A.; Tarasova, N. N. *Izv. Timiryazevsk. S'kh. Akad.* **1956**, 183–190.
(9) Khitrova, N. N.; Khitrov, V. A. *Izv. Sekt. Fiz.-Khim. Anal., Inst. Obshch. Neorg. Khim., Akad. Nauk SSSR* **1956**, *27*, 328–336.

Received for review August 27, 1987. Accepted March 15, 1988.